

A new index of glacier area change: a tool for glacier monitoring

Mark DYURGEROV,^{1,2} Mark F. MEIER,¹ David B. BAHR³

¹*Institute of Arctic and Alpine Research, UCB 450, University of Colorado at Boulder, Boulder, Colorado 80309-0450, USA*
E-mail: dyurg@tintin.colorado.edu

²*Department of Physical Geography and Quaternary Geology, Stockholm University, SE-106 91 Stockholm, Sweden*

³*Department of Physics and Computational Science, Regis University, Denver, Colorado 80221, USA*

ABSTRACT. Since the mid-19th century, most glaciers have been losing area and volume. This loss of area has not been homogeneous in time and space, and direct observations are sparse, making regional and global estimates of glacier change difficult. This paper focuses on developing a single index for monitoring glacier change, one that would be particularly useful for remote-sensing applications. We combine the results of direct glacier mass-balance observations B , total glacier area S and accumulation area S_c derived from maps or remotely sensed images. Using the accumulation–area ratio ($AAR = S_c/S$), we note the differences between observed AAR, time-averaged $\langle AAR \rangle$ and the equilibrium state AAR_0 , as determined by its value at $B = 0$ from a regression of $B(AAR)$. We suggest that $\alpha_d = (\langle AAR \rangle - AAR_0)/AAR_0$ quantifies the difference between the currently observed state of glaciers and their equilibrium state and measures the delay in the dynamic response of S relative to the climatic response of S_c . Using all available observations for the period 1961–2004, $\alpha_d \approx -65\%$ for tropical glaciers, which implies their rapid shrinkage as S continues to decrease and ‘catch up’ with S_c . During the same period, mid-latitude and polar glaciers show less negative values of α_d . Of 86 glaciers from all latitudes and regions, only 11 show positive α_d at any time between 1961 and 2004. Averaged over 1961–2004, α_d is $-15.1 \pm 2.2\%$, and $\langle B \rangle$ is $-360 \pm 42 \text{ mm a}^{-1}$ w.e. Values for AAR_0 range between about 40% and 80%, but the bulk of the equilibrium values are between 50% and 60%. The average AAR_0 is $57.9 \pm 0.9\%$ and has remained stable over time (the equilibrium AAR has not changed with climate). Overall, the observed negative α_d suggests a committed retreat of glaciers and their continuing contribution to sea level even if global temperature is held constant.

INTRODUCTION

Glaciers and ice caps, exclusive of the Greenland and Antarctic ice sheets, contribute substantially to sea-level rise (Meier and others, 2007; Bahr and others, 2009). In recent decades, all around the world, these glaciers and ice caps (referred to as ‘glaciers’ in this paper) have rapidly disintegrated (Oerlemans and others, 2007). These changes have not been homogeneous in time and space; growth and shrinkage have been observed simultaneously in different regions and at different time periods, making regional and global estimates of glacier change complicated. Furthermore, the large number of glaciers and their generally inaccessible locations require satellite or airborne remote sensing to monitor changes on a regional or global basis (Raup and others, 2007). This paper focuses on developing a simple and widely applicable measure of glacier changes that will be especially useful for observations over large areas using remote sensing.

Previous observations show that the accumulation–area ratio ($AAR = S_c/S$, where S_c is accumulation area and S is the total glacier area) changes in concert with annual (or net) glacier mass balance B (Dyurgerov and Meier, 2005). This relationship suggests that the change in glacier accumulation areas can be quantified in relation to mass-balance changes and, to a certain extent, climate change, due to a statistically significant inverse relationship between B and annual global mean air temperature (Oerlemans, 2001). This relationship has a physical background, as mass balance is generally a function of altitude, and the equilibrium-line altitude (ELA) separates the accumulation area (above) from the rest of the glacier (below). Air

temperature and thus ice- and snowmelt rates generally decrease, and snow accumulation rates generally increase, with altitude. Thus ELA, AAR and B are related (Shumsky, 1947; Meier and Post, 1962). We use this relationship to develop a single index for monitoring glacier changes.

CONCEPT

The index is defined as the difference between two states of AAR for a glacier. One state is determined by averaging the observed time-varying AAR_i (where i is the year). We write this time average as $\langle AAR \rangle$. The second is a glacier’s hypothetical equilibrium AAR_0 which is the accumulation–area ratio of the glacier if and when it is in mass-balance equilibrium. In particular, the equilibrium state, AAR_0 , is the value of AAR at $B = 0$ in a regression of AAR_i against B_i . Note that when making these averages and regressions for different glaciers, the periods of observations (ranges of i) will vary; this is a serious deficiency in mass-balance observations. It is impossible to compile a large sample of glaciers with both AAR data and simultaneous B data that all fall within the same range of years. Even so, the relationship between all mass-balance and AAR glacier time series is significant, with $R^2 = 0.55$ (Fig. 1; data presented in Table 1). The $\alpha_d = (\langle AAR \rangle - AAR_0)/AAR_0$ measures a glacier’s displacement from equilibrium and is a relatively simple index for monitoring glacier change that directly relates changes in mass balance B , ELA and accumulation area size S_c . Note that α_d represents an undelayed response to change in water and energy-balance components, whereas the change of the entire glacier

area S , which occurs mainly below the ELA, is a delayed adjustment to mass-balance and climate change. Positive values of α_d suggest that a glacier's accumulation area, and probably also its total area, have been expanding over the period of observations. Negative values of α_d suggest that a glacier has been or will be in retreat, thus probably decreasing S_c and S . Note that in general, S_c has been decreasing in recent years (e.g. Haeberli and others, 2007). Thus, glaciers have an increasing deficit of accumulation area, closely related to climate warming (Dyurgerov, 2007).

Equivalently, the index α_d could be written as a ratio $\alpha_r = \langle \text{AAR} \rangle / \text{AAR}_0$ (Bahr and others, 2009). These two formulations are linearly related and can therefore be used interchangeably. In some applications, the ratio α_r gives a more convenient measure of the percentage by which a glacier is out of equilibrium, and Bahr and others (2009) use this metric in a scaling analysis to estimate possible future changes in glacier volume and consequent sea-level rise. In other situations, the difference represented by α_d gives a more convenient measure of the actual change in AAR necessary for a glacier to reach equilibrium. The choice of α_d or α_r will depend on the application, and, because the formulations are otherwise equivalent, we reference only α_d in the remainder of this paper.

In order to use α_d (or α_r) as a quantitative measure of the observed state of glaciers relative to their equilibrium state, each glacier's AAR and AAR_0 must be accurately observed or otherwise precisely determined. The major difficulty with existing AAR data is that the time series are incomplete, and no information on data accuracy has been reported in many publications. In the next section, we compile and analyze published AAR data with these constraints in mind.

DATA SOURCES

The results of this study are based on available time series of B_i , S_i , S_{ci} and ELA_i for 99 glaciers from around the world during the time period 1961–2004 (Table 1). These data are mostly derived from *Fluctuations of glaciers* (e.g. WGMS, 2005) and the *Glacier Mass Balance Bulletin* (e.g. WGMS, 2007), available at the website <http://www.wgms.ch>. The continuous time series of the above variables were also compiled in two reports (Dyurgerov, 2002; Dyurgerov and Meier, 2005). AAR values are usually derived from glacier hypsometry and the mass-balance vs altitude function using ELA data (e.g. Kjølmoen and others, 2006). In all, more than 200 annual time series were examined, and 99 time series with records of 5 years or longer were chosen for analysis.

These data are taken from observations spanning almost 50 years. The glacier surface area S_i changes with time and represents the 'conventional' area as defined by Elsberg and others (2001). The direct mass-balance method (Mayo and others, 1972), with many modifications (Østrem and Brugman, 1991), has been used for most observations. Some changes in methods and observing teams have occurred since observations began, so the time series may not be homogeneous (e.g. Storglaciären in Scandinavia (Holmlund and others, 2005; R. Hock and others, unpublished information)). Non-homogeneity is a common source of uncertainty, which can only be estimated for a few glaciers.

Outliers were subjected to credibility assessment. The AAR data were sometimes found to be different in various publications (e.g. institutional reports, such as from the

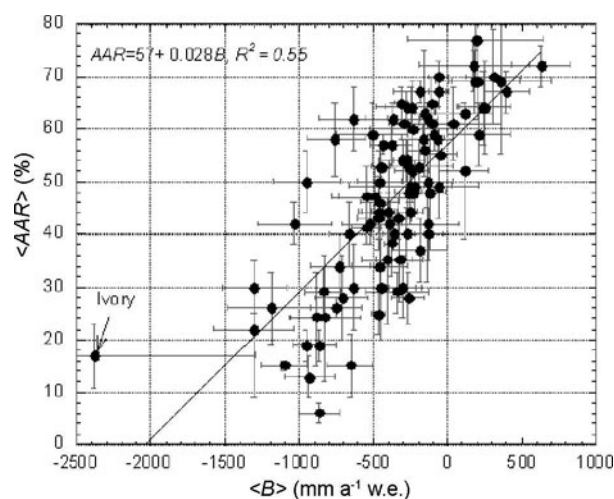


Fig. 1. The relationship between average mass balance $\langle B \rangle$ and average accumulation–area ratio $\langle \text{AAR} \rangle$ ($R^2 = 0.55$). Each point on the regression is the time average for one of the ninety-nine glaciers listed in Table 1, with time series from 5 to 45 years covering the period 1961–2004. Bars indicate the standard errors. The largest outlier is Ivory Glacier, New Zealand.

Norwegian Water Resources and Energy Directorate (NVE) or United States Geological Survey (USGS), compared to World Glacier Monitoring Service (WGMS) reports). Such data were excluded from the series or corrected by comparisons with the ELA results, where available. For all cases where the ELA is above the glacier's highest elevation or below its lowest elevation, the AAR results are excluded from further analysis. This is a limitation of the method, especially when applied to a very small glacier where the ELA occasionally varies above and below the glacier (e.g. Glacier Zongo in the Andes).

RELATIONSHIP BETWEEN AAR AND MASS BALANCE

All 99 available time series of AAR_i were regressed against their respective B_i . The relationship between B and AAR is generally strong and linear (Fig. 2a). However, in some cases a linear regression is inappropriate.

Linear regression of AAR vs B. The majority of all regressions show a linear relation (69 of 99 glaciers) (e.g. Fig. 2a).

Non-linear regression of AAR vs B. A minority of the glaciers have non-linear regressions (e.g. Fig. 2b and c). We suggest that some of these non-linear regressions are caused by anomalous increases or decreases in snow accumulation in the upper or lower parts of the glaciers. Non-linearity has also been observed for some glaciers in maritime climates where glacier mass balance and volume change vs elevation are more sensitive to changes in the amount of snow accumulation (e.g. coastal Norway; Iceland). In general, these non-linear regressions can be best summarized as concave-down (e.g. Nigardsbreen in Scandinavia (Fig. 2b)) and concave-up (e.g. Wurtenees in the European Alps (Fig. 2c)).

Large outliers with no regression. There are several cases with no statistically significant relationships between AAR and B . These may be related to the complicated basin topography and the resulting complex glacier shapes that

Table 1. Glacier data used in this analysis. $\langle B \rangle$ indicates an average over time and is measured in mm w.e.; $\langle AAR \rangle$ indicates an average over time and is measured in %; sterr is standard error = std dev. $\times N^{-1/2}$; years is the number of years of record; AAR_0 and α_d (%) are defined in the text

Glacier	Lat.	Long.	$\langle B \rangle$	$\langle B \rangle$ sterr	$\langle AAR \rangle$	Years	$\langle AAR \rangle$ sterr	AAR_0	α_d
White*	79°27' N	90°40' W	-112	35	61	42	3	71	-14.1
Baby	79°26' N	90°58' W	-159	69	63	10	12	65	-3.1
Devon Ice Cap northwest	75°25' N	83°15' W	-86	25	59	37	3	71	-16.8
Alexander	57°06' N	130°49' W	-716	184	28	8	8	58	-51.4
Andrei	56°56' N	130°59' W	-456	133	46	9	5	59	-21.3
Yuri	56°58' N	130°41' W	-629	203	31	8	8	53	-41.5
Bench	51°26' N	124°55' W	-660	141	41	6	6	65	-37.7
Helm	49°58' N	123°00' W	-1299	215	30	19	5	45	-33.3
Place	50°26' N	122°36' W	-840	124	29	27	5	51	-43.1
Sentinel	49°54' N	122°59' W	245	183	65	24	7	56	15.3
Tiedemann	51°20' N	125°03' W	-1027	245	n.incl.		4	n.incl.	
Zavisha	50°48' N	123°25' W	-139	216	42	10	11	49	-14.3
Peyto*	51°40' N	116°32' W	-547	102	41	28	3	54	-24.1
Ram River	51°51' N	116°11' W	-408	169	35	5	12	56	-37.5
Blue*	47°49' N	123°41' W	-170	145	58	40	3	61	-4.9
Columbia	47°58' N	121°21' W	-307	164	54	5	4	68	-20.6
Foss	47°33' N	121°12' W	-279	196	64	5	3	65	-1.5
Ice Worm	47°50' N	121°10' W	-490	247	47	5	6	68	-30.9
Lower Curtis	48°48' N	121°37' W	-384	145	57	5	4	70	-18.6
Lynch	48°39' N	121°11' W	-189	176	67	5	2	69	-2.9
Rainbow	48°48' N	121°46' W	-243	179	64	5	4	66	-3.0
South Cascade	48°22' N	121°03' W	-468	137	43	22	6	53	-18.9
Gulkana*	63°14' N	145°28' W	-298	103	61	39	1	66	-7.6
McCall	69°17' N	143°50' W	-393	82	42	12	4	57	-26.3
Wolverine*	60°22' N	148°54' W	-370	189	62	37	3	65	-4.6
Chacaltaya	16°21' S	68°07' W	-1305	271	22	7	13	64	-65.6
Zongo	16°15' S	68°10' W	-505	240	59	14	6	68	-13.2
Antizana	0°29' S	79°09' W	-635	228	62	7	6	65	-4.6
Blagnipujökull	64°43' N	19°03' W	-338	214	29	11	4	56	-48.2
Dyngjujökull	64°40' N	17°00' W	177	373	72	5	5	59	22.0
Satujökull	64°55' N	18°50' W	-524	184	42	12	4	48	-12.5
Þjórsárjökull	64°48' N	18°35' W	-550	233	47	11	6	52	-9.6
Tungnaarjökull	64°19' N	18°04' W	-951	228	50	8	6	62	-19.4
Austre Brøggerbreen*	78°53' N	11°50' E	-468	51	25	35	4	58	-56.9
Kongsvegen	78°48' N	12°59' E	-64	97	49	14	6	50	-2.0
Midre Lovénbreen	78°53' N	12°04' E	-378	51	38	15	6	55	-30.9
Hans	77°05' N	15°40' E	-726	203	34	10	6	52	-34.6
Engabreen	66°40' N	13°45' E	632	192	72	30	4	60	20.0
Svartisheibreen	66°35' N	13°45' E	203	285	69	8	7	65	6.2
Austre Okstnbreen	66°14' N	14°22' E	115	198	n.incl.		2	n.incl.	
Trollbergdalsbreen	66°43' N	14°27' E	-450	277	30	7	10	43	-30.2
Hogtubvreen	66°27' N	13°39' E	41	320	61	5	7	60	1.7
Langfjordjökelen	70°10' N	21°45' E	-756	201	n.incl.		7	n.incl.	
Storsteinsfjellbreen	68°13' N	17°55' E	307	184	70	10	9	47	48.9
Alftobreen*	61°45' N	5°39' E	210	212	59	42	6	53	11.3
Hansebreen	61°45' N	5°41' E	-383	293	n.incl.		9	n.incl.	
Storbreen*	61°34' N	8°08' E	-262	87	48	56	4	57	-15.8
Hellstugubreen*	61°34' N	8°26' E	-335	94	43	43	4	55	-21.8
Hardangerjökelen	60°32' N	7°22' E	125	160	72	41	13	65	7.0
Gråsubreen	61°39' N	8°36' E	-306	91	30	43	6	46	-34.8
Nigardsbreen*	61°43' N	7°08' E	400	157	67	43	4	65	3.1
Austdalsbreen	61°48' N	7°21' E	-232	291	60	17	9	70	-14.3
Marmaglaciären	68°05' N	18°41' E	-267	111	28	14	5	36	-22.2
Riukojietna	68°05' N	18°05' E	-403	194	44	18	10	52	-15.4
Tarfala	67°56' N	18°39' E	356	344	69	7	14	61	13.1
Karsojietna	68°21' N	18°19' E	189	160	69	7	6	51	35.3
Storglaciären	67°54' N	18°34' E	-257	94	44	58	2	46	-4.3
Rabots	67°54' N	18°33' E	-276	119	40	20	5	50	-20.0
Limmern	46°49' N	8°59' E	-122	108	48	42	8	51	-5.9
Plattalva	46°50' N	8°59' E	-119	110	48	42	11	48	0.0
Gries*	46°26' N	8°20' E	-404	118	44	43	4	57	-22.8
Silvretta*	46°51' N	10°05' E	-49	111	55	45	5	57	-3.5
Hintereisferner*	46°48' N	10°46' E	-445	75	53	49	3	69	-23.2
Kesselwandferner*	46°50' N	10°48' E	-63	67	67	47	3	74	-9.5
Vernagtferner*	46°53' N	10°49' E	-278	86	54	40	4	67	-19.4

Table 1. Continued

Glacier	Lat.	Long.	$\langle B \rangle$	$\langle B \rangle$ sterr	$\langle AAR \rangle$	Years	$\langle AAR \rangle$ sterr	AAR ₀	α_d
Filleckkees	47°08' N	12°36' E	252	174	64	17	9	60	6.7
Sonnblickkees*	47°08' N	12°36' E	-263	125	53	46	5	59	-10.2
Wurtenkees	47°02' N	13°00' E	-867	115	19	22	3	43	-55.8
Jamtalferner	46°42' N	10°10' E	-657	152	n.incl.		6	n.incl.	
Vermuntgletscher	46°51' N	10°08' E	-932	172	n.incl.		4	n.incl.	
Ochsentaler	46°51' N	10°06' E	-458	158	50	9	6	67	-25.4
Langtaler	46°48' N	11°01' E	-192	226	53	8	5	57	-7.0
Ciardoney	45°31' N	7°26' E	-1184	300	26	13	7	57	-54.4
Careser	46°27' N	10°42' E	-869	136	n.incl.		2	n.incl.	
Sforzellina	46°20' N	10°30' E	-949	97	n.incl.		3	n.incl.	
Fontana Bianca	46°29' N	10°46' E	-752	175	n.incl.		2	n.incl.	
Pendente	46°52' N	10°14' E	-825	235	24	9	12	50	-52.0
Maladeta	42°39' N	0°38' E	-459	191	34	13	5	40	-15.0
Lewis	0°09' S	37°18' E	-890	180	24	18	9	68	-64.7
Djankuat*	43°12' N	42°46' E	-66	105	58	36	2	59	-1.7
Garabashi	43°18' N	42°28' E	-157	117	56	20	5	62	-9.7
Marukh	43°05' N	41°10' E	-321	157	35	16	8	42	-16.7
Leviy Aktru	50°05' N	87°44' E	-134	63	62	28	2	63	-1.6
Maliy Aktru*	50°05' N	87°45' E	-62	66	70	43	3	71	-1.4
No. 125	50°06' N	87°42' E	-107	54	65	28	5	71	-8.5
Kozelskiy	53°14' N	158°49' E	-251	204	49	25	5	55	-10.9
IGAN	67°40' N	65°80' E	-187	187	37	24	6	42	-11.9
Obrucheva	67°43' N	65°70' E	-134	175	50	24	5	52	-3.8
Abramov*	39°40' N	71°30' E	-457	115	44	31	4	55	-20.0
Tsentralny Tuyuksuyskiy*	43°00' N	77°06' E	-366	70	40	48	3	55	-27.3
Kara-Batkak	42°06' N	78°18' E	-438	62	n.incl.		2	n.incl.	
Golubina	42°27' N	74°30' E	-312	43	65	26	3	73	-11.0
Sary-Tor	41°50' N	78°11' E	-125	95	40	6	5	45	-11.1
Ürümqi No. 1*	43°05' N	86°49' E	-231	53	48	46	2	55	-12.7
Changme-Khangpu	27°57' N	88°41' E	-242	113	n.incl.		2	n.incl.	
Dunagiri	30°33' N	79°54' E	-1097	156	n.incl.		1	n.incl.	
Shaune Garang	31°17' N	78°20' E	-226	440	49	9	5	56	-12.5
Xiao Dongkemadi	33°10' N	92°08' E	194	458	77	10	9	64	20.3
Ivory	43°08' S	170°55' E	-2383	1093	n.incl.		6	n.incl.	
Number of records			99						86
Average			-360	174	49.2		5.5	57.9	-15.1
Standard deviation			425	125	14.2		2.9	8.7	20.6
Standard error			42		1.4		0.3	0.9	2.2

*Glaciers used to calculate trends in area change in Figure 3.

Note: Some glaciers could not be assigned AAR₀, as discussed in the text (denoted here as 'n.incl.').

affect snow-cover distribution. As a result, the spatial distribution of snow accumulation patterns does not show clear dependencies on elevation. Time series may also be short or AAR(B) may cover a limited range of AAR, so the relationship between AAR and B may not be reliable (e.g. Dunagiri and Changme-Khangpu glaciers in the Himalaya, Gråsubreen in Scandinavia, Kara-Batkak glacier in the Tien Shan, and Ivory Glacier in New Zealand (Fig. 2d; data in Table 1)). In these cases, the equilibrium state cannot be defined accurately, and 13 glaciers were removed from further analysis (these are indicated in Table 1 as 'n.incl.' or not included). A few glaciers with tongues calving in water (e.g. northwestern part of Devon Ice Cap in the Canadian Arctic, and Austdalsbreen in Scandinavia) show AAR₀ of about 70% or more because part of the ablation is by iceberg calving. AAR and B observations are very sparse for tidewater glaciers and outlets from ice caps, but the application of α_d to these glaciers deserves further investigation. Time series of mass balances and corresponding AAR for the 86 remaining glaciers were subjected to further analysis.

AAR₀ has been computed for each glacier by using a linear or higher-order polynomial regression with a least-squares fit. To choose which regression should be used to calculate AAR₀ from the empirical data, the test $3\sigma \geq [AAR_0 \text{ (linear)} - AAR_0 \text{ (polynomial)}]$ has been applied, where σ is the standard deviation of observed AAR. Based on this test, a higher-order polynomial regression of AAR₀ was adopted for 11 glaciers. The standard errors of AAR and mass balance are given in Table 1 (σ/\sqrt{n} , where n is the number of time series).

RESULTS

Based on the data analysis and calculations of α_d , several results stand out.

1. The widespread decreases in AAR appear to be due to rapid decreases in S_c relative to slower decreases of S (Fig. 3). Large changes in S_c may have resulted from quite small changes in the ELA because the area distribution

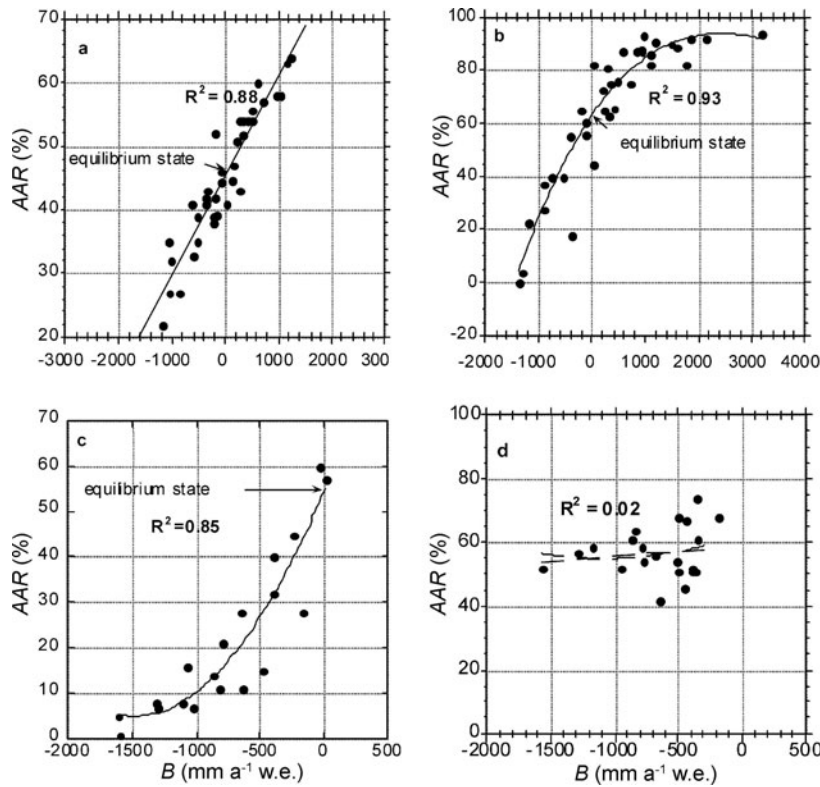


Fig. 2. Examples of the relationship between AAR_i and B_i for different glaciers, showing (a) a linear regression (most common) (Storglaciären); (b) a higher-order polynomial regression with a concave-down relationship (Nigardsbreen); (c) a higher-order polynomial regression with a concave-up relationship (Wurtenkees); and (d) no significant relationship (Kara-Batkak). Each point is for a different year *i*.

(versus elevation) is generally largest above the average ELA. Changes in *S* occur more slowly as the glacier adjusts dynamically to climate and mass-balance changes.

2. Faster decreases in *S_c* compared to *S* suggest that glaciers are committed to further retreat even if the climate were to stop changing. While changes to *S_c* could cease

immediately, the ongoing dynamic response will cause continuing changes in glacier area *S*. If this committed retreat ($\alpha_d = -15.1 \pm 2.2\%$) applies to all glaciers and ice caps, with total area about $763 \times 10^3 \text{ km}^2$ (Meier and others, 2007), the total glacier area has to decrease by about $115 \times 10^3 \text{ km}^2$. This decrease is apparently under way.

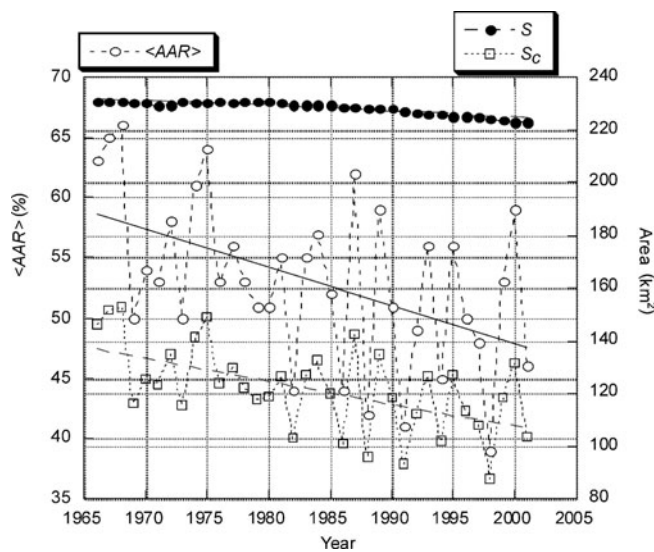


Fig. 3. The change in total area *S* and accumulation area *S_c* summed annually for 22 Northern Hemisphere glaciers during 1966–2001. These glaciers are designated by asterisks in Table 1. The trend lines show that *S* was decreasing at a rate of $-0.21 \text{ km}^2 \text{ a}^{-1}$ and *S_c* was decreasing at a rate of $-0.87 \text{ km}^2 \text{ a}^{-1}$.

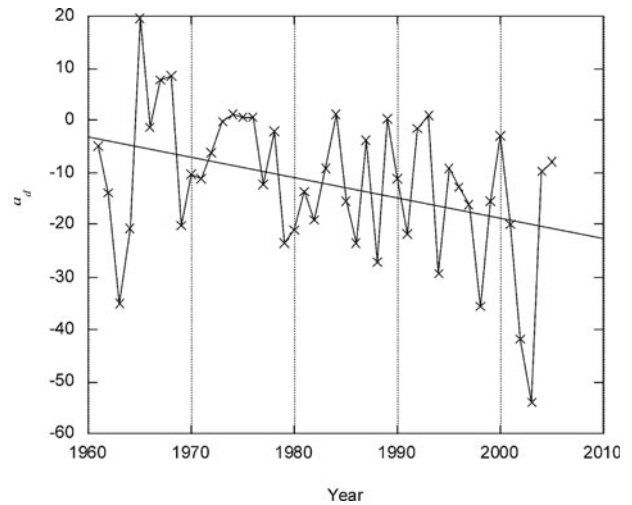


Fig. 4. The change with time of α_d . For each glacier, a value for α_d was calculated for each year (AAR_i were calculated from annual observational data and AAR₀ was estimated from a linear or higher-order polynomial fit to the observed relationship between AAR_i and B_i). Each point on the plot is the average α_d for all of the glaciers in the given year. The trend is $-0.39\% \text{ a}^{-1}$.

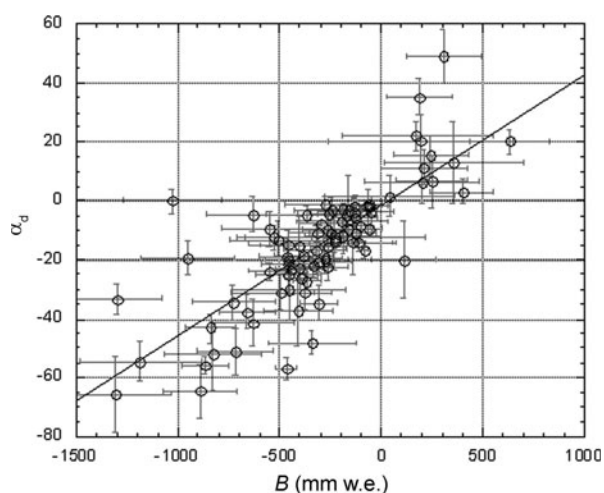


Fig. 5. The relationship between α_d and average mass balance $\langle B \rangle$ ($R^2 = 0.6$). Each point represents an average for each of the 86 glaciers that can be assigned a value for α_d (Table 1). Averages are over the period of observation, 1961–2004, though most glaciers do not have data available for each year. Standard error bars are shown.

- α_d is decreasing with time (Fig. 4) due to decreasing globally averaged glacier mass balance (e.g. Kaser and others, 2006) and increasing ELA (Dyurgerov and Meier, 2005).
- The sample of glaciers available for analysis shows that negative α_d are dominant (Table 1). A majority of glaciers in the sample are far from a steady state and need to shrink to reach equilibrium with the recent climate. The largest negative α_d values are about -66% and -65% for the tropical glaciers Chacaltaya in South America and Lewis in East Africa respectively. These deficits suggest the forthcoming disappearance of many glaciers in the tropics (Hastenrath and Greischar, 1997; Kaser and Osmaston, 2002). Mid-latitude and polar glaciers show less negative α_d values (Table 1).
- Some glaciers have a positive α_d , indicating that they need to expand their area by advancing. The maximum value is 49% for Storsteinsfjellbreen in Scandinavia. Of 86 glaciers, 13 show positive mass balances (Fig. 5). These include 10 in Scandinavia, Sentinel Glacier in the Canadian Coast Ranges, Filleckees in the European Alps, and Dyngjufjökull, the periodically surging outlet of Vatnajökull in Iceland. Averaged over 86 time series for the entire 1961–2004 period, α_d is $-15.1 \pm 2.2\%$, and averaged for 99 glaciers B is $-360 \pm 42 \text{ mm a}^{-1} \text{ w.e.}$ (Table 1). These averages, however, are over a long period, when most glacier balances were changing from near-equilibrium toward markedly negative values.
- The calculated AAR_0 show differences ranging from about 40% up to 80% for individual glaciers, as noted before (Meier and Post, 1962). The most frequent values of AAR_0 in the sample used here are $50\text{--}60\%$, with an average value of $57.9 \pm 0.9\%$ (Table 1), the same as determined theoretically for mountain glaciers by Bahr (1997).
- The equilibrium AAR_0 has not changed with time. The results shown in Figure 6 might suggest a slight decrease of AAR_0 with time, but applying the t -criteria between averaged AAR_0 for the periods 1961–75, 1976–90 and

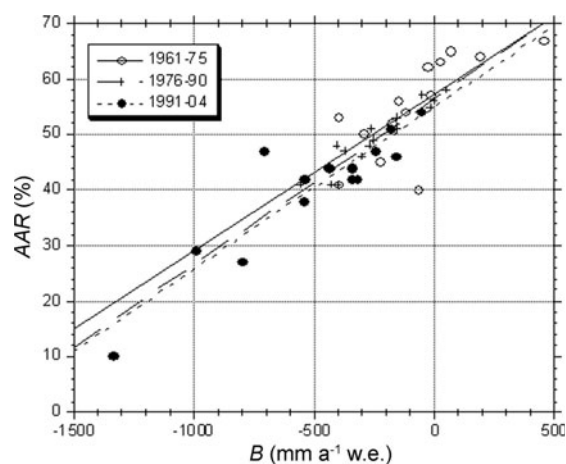


Fig. 6. The relationship between AAR and B for several different time intervals. Each point is the average AAR and average B for all glaciers in the dataset (Table 1) for a particular year. For 1961–75, the average (over all open circles) is $\langle \text{AAR} \rangle = 54\%$ and $\langle B \rangle = -113 \text{ mm a}^{-1} \text{ w.e.}$ ($R^2 = 0.6$). For 1976–90, the average (over all crosses) is $\langle \text{AAR} \rangle = 49\%$ and $\langle B \rangle = -238 \text{ mm a}^{-1} \text{ w.e.}$ ($R^2 = 0.89$). For 1991–2004, the average (over all filled circles) is $\langle \text{AAR} \rangle = 40\%$ and $\langle B \rangle = -491 \text{ mm a}^{-1} \text{ w.e.}$ ($R^2 = 0.83$). Corresponding to these same time intervals, the average AAR_0 changed from 57.2% to 56.6% to 54.9% . For the entire 1961–2004 period (regression not shown), the average $\text{AAR}_0 = 57.9\%$, $\langle \text{AAR} \rangle = 47\%$ and $\langle B \rangle = -360 \text{ mm a}^{-1} \text{ w.e.}$

1991–2004 shows that the differences are not significant at the 0.95 significance level. The Hydrologic Encyclopedia volume 1 (Anderson and others, 2005, p. 387) gives the number for ‘Glacier equilibrium line area’ 0.65, which means AAR balanced. Our calculation gives 58% , which we recommend for use in paleoclimatic studies (e.g. in conjunction with reconstructions from trimlines and moraines).

- We also calculated AAR_{0i} using the average of all available AAR_i and B_i for all glaciers for each year i . These annual estimates of AAR_{0i} (averaged over all glaciers) ranged between 50.3% (in 1992) and 60.6% (in 1986).

CONCLUSIONS

Changes in glaciers can be monitored with the index α_d . The index may be particularly useful with remotely sensed ELA and/or AAR data (S_c and S can be determined remotely, with some known limitations) along with standard mass-balance observations. α_d quantifies the extent to which a glacier is out of equilibrium. The index α_d (and equivalently α_r) can be used in applications that need to know the extent to which glaciers are out of equilibrium, as has been done, for example, when calculating glacier contributions to sea level (Bahr and others, 2009). The index also suggests that $\text{AAR}_0 = 57.9 \pm 0.9\%$ is an appropriate AAR for steady-state glaciers and this value should be used in paleo-glacier and paleoclimate reconstructions (instead of the more commonly used 66%).

Using α_d , our data show that the majority of glaciers are far from steady state and need to shrink to reach equilibrium with the recent climate (which can be monitored by the size of S_c). Faster decreases in S_c compared to S reflect the direct and undelayed response of glacier mass balance to climate

warming. The delayed dynamic response of S suggests that the glaciers are committed to further retreat, even if the climate stops changing. With a worldwide total of $763 \times 10^3 \text{ km}^2$ of glacier area, the committed retreat will cause that total to decrease by $115 \times 10^3 \text{ km}^2$ before equilibrium can be re-established. This process is underway. Thus, even if the climate stops changing and does not become warmer, glaciers will continue to retreat.

ACKNOWLEDGEMENTS

This work was supported by the US National Science Foundation (OPP/ANS-0425488) and a Marie Curie International Fellowship within the 6th European Community Framework Program. M. Dyurgerov also acknowledges financial support for this study from the Swedish Research Council (VR) and that the study has partly been carried out within the Bert Bolin Centre for Climate Research at Stockholm University, which is supported by a joint Linnaeus grant from the research councils Formas and VR. We are grateful to R. Hock, A. Arendt and G. Cogley for making many useful comments on the manuscript.

REFERENCES

- Anderson, M.G. and J.J. McDonnell. 2005. *Encyclopedia of hydrological sciences*. Vol. 1. New York, etc., Wiley.
- Bahr, D.B. 1997. Width and length scaling of glaciers. *J. Glaciol.*, **43**(145), 557–562.
- Bahr, D.B., M. Dyurgerov and M.F. Meier. 2009. Sea-level rise from glaciers and ice caps: a lower bound. *Geophys. Res. Lett.*, **36**(3), L3501. (10.1029/2008GL036309.)
- Dyurgerov, M. 2002. *Glacier mass balance and regime: data of measurements and analysis*. Boulder, CO, University of Colorado. Institute of Arctic and Alpine Research. (INSTAAR Occasional Paper 55.)
- Dyurgerov, M. 2007. Glacier monitoring approach suggested from analysis of mass balance observations. In Oerlemans, J. and C.H. Tilm-Reijmer, eds. *The dynamics and mass budget of Arctic glaciers. Extended abstracts. Workshop and GLACIODYN (IPY) Meeting, 15–18 January 2007, Pontresina, Switzerland*. Utrecht, Utrecht University. Institute for Marine and Atmospheric Research Utrecht, 37–39.
- Dyurgerov, M.B. and M.F. Meier. 2005. *Glaciers and the changing Earth system: a 2004 snapshot*. Boulder, CO, University of Colorado. Institute of Arctic and Alpine Research. (INSTAAR Occasional Paper 58.)
- Elsberg, D.H., W.D. Harrison, K.A. Echelmeyer and R.M. Krimmel. 2001. Quantifying the effects of climate and surface change on glacier mass balance. *J. Glaciol.*, **47**(159), 649–658.
- Haeblerli, W., M. Hoelzle, F. Paul and M. Zemp. 2007. Integrated monitoring of mountain glaciers as key indicators of global climate change: the European Alps. *Ann. Glaciol.*, **46**, 150–160.
- Hastenrath, S. and L. Greischar. 1997. Glacier recession on Kilimanjaro, East Africa, 1912–89. *J. Glaciol.*, **43**(145), 455–459.
- Holmlund, P., P. Jansson and R. Pettersson. 2005. A re-analysis of the 58 year mass-balance record of Storglaciären, Sweden. *Ann. Glaciol.*, **42**, 389–394.
- Kaser, G. and H. Osmaston. 2002. *Tropical glaciers*. Cambridge, etc., Cambridge University Press.
- Kaser, G., J.G. Cogley, M.B. Dyurgerov, M.F. Meier and A. Ohmura. 2006. Mass balance of glaciers and ice caps: consensus estimates for 1961–2004. *Geophys. Res. Lett.*, **33**(19), L19501. (10.1029/2006GL027511.)
- Kjøllmoen, B., L.M. Andreassen, R.V. Engeset, H. Elvehøy, M. Jackson and R.H. Giesen. 2006. Glaciological investigations in Norway in 2005. *NVE Rapp.* 2-2006.
- Mayo, L.R., M.F. Meier and W.V. Tangborn. 1972. A system to combine stratigraphic and annual mass-balance systems: a contribution to the International Hydrological Decade. *J. Glaciol.*, **11**(61), 3–14.
- Meier, M.F. and A.S. Post. 1962. Recent variations in mass net budgets of glaciers in western North America. *IASH Publ.* 58 (Symposium at Obergurgl 1962 – *Variations of the Regime of Existing Glaciers*), 63–77.
- Meier, M.F. and 7 others. 2007. Glaciers dominate eustatic sea-level rise in the 21st century. *Science*, **317**(5841), 1064–1067.
- Oerlemans, J. 2001. *Glaciers and climate change*. Lisse, etc., A.A. Balkema.
- Oerlemans, J., M. Dyurgerov and R.S.W. van de Wal. 2007. Reconstructing the glacier contribution to sea-level rise back to 1850. *Cryosphere*, **1**(1), 59–65.
- Østrem, G. and M. Brugman. 1991. *Glacier mass-balance measurements. A manual for field and office work*. Saskatoon, Sask., Environment Canada. National Hydrology Research Institute. (NHRI Science Report 4.)
- Raup, B., A. Racoviteanu, S.J.S. Khalsa, C. Helm, R. Armstrong and Y. Arnaud. 2007. The GLIMS geospatial glacier database: a new tool for studying glacier change. *Global Planet. Change*, **56**(1–2), 101–110.
- Shumsky, P.A. 1997. The energy of glacierization and the life of glaciers. In Kotlyakov, V.M., ed. *34 selected papers on main ideas of the Soviet glaciology, 1940s–1980s*. Moscow, Glaciological Association, 19–43.
- World Glacier Monitoring Service (WGMS). 2005. *Fluctuations of glaciers 1995–2000 (Vol. VIII)*, ed. W. Haeblerli, M. Zemp, R. Frauenfelder, M. Hoelzle and A. Käbb. IAHS/UNEP/UNESCO, World Glacier Monitoring Service, Zürich.
- WGMS. 2007. *Glacier Mass Balance Bulletin No. 9 (2004–2005)*, ed. Haeblerli, W., M. Hoelzle and M. Zemp. Zürich, ICSU (FAGS)/IUGG(IACS)/UNEP/UNESCO/WMO, World Glacier Monitoring Service.

MS received 23 October 2008 and accepted in revised form 7 May 2009